How to cite: *Angew. Chem. Int. Ed.* **2021**, *60*, 10393–10401
International Edition: doi.org/10.1002/anie.202014822
German Edition: doi.org/10.1002/ange.202014822

Inorganic Crown Ethers

Construction of Inorganic Crown Ethers by s-Block-Metal-Templated Si–O Bond Activation

Fabian Dankert, Roman-Malte Richter, Florian Weigend, Xiulan Xie, Markus Balmer, and Carsten von Hänisch**

Abstract: *We herein report the synthesis, structures, coordination ability, and mechanism of formation of silicon analogs of crown ethers. An oligomerization of $^2D_2$ (**I**) ($^2D_n = (Me_4Si_2O)_n$) was achieved by the reaction with GaI_3 and MI_x ($M = Li, Na, Mg, Ca, Sr$). In these reactions the metal cations serve as template and the anions ($I^-/[GaI_4]^-$) are required as nucleophiles. In case of $MI_x = LiI$, $[Li(^2D_3)GaI_4]$ (**1**) is formed. In case of $MI_x = NaI$, MgI_2, CaI_2, and SrI_2 the compounds $[M(^2D_4)(GaI_4)_x]$ ($M = Mg^{2+}$ (**3**), Ca^{2+} (**4**), Sr^{2+} (**5**) are obtained. Furthermore the proton complex $[H(^2D_3)][Ga_2I_7]$ (**6**) was isolated and structurally characterized. All complexes were characterized by means of multinuclear NMR spectroscopy, DOSY experiments and, except for compound **3**, also by single crystal X-ray diffraction. Quantum chemical calculations were carried out to compare the affinity of M^+ to ^2D_n and other ligands and to shed light on the formation of larger rings from smaller ones.*

Introduction

Since their discovery in the mid-sixties, crown ethers and related compounds such as cryptands, spherands, and podands came a long way. Due to their fantastic coordination ability, they were reviewed several times, gained many fields of applications and it was in 1987 when C. J. Pedersen, J. M. Lehn and D. J. Cram were awarded with the Nobel prize in chemistry for their research in supramolecular chemistry.[1–5] However, much less attention was paid to silicon analogues of crown ethers even though there has been a major interest in "inorganic" macrocycles over the years.[6–15] Furthermore, many works of the last few decades dealt with the Si-imitation of organic chemistry: Compounds were characterized which represent silicon–silicon multiple bonds,[16–20] silanones[21–23] silanoic esters,[24,25] silacarboxylates,[26] silanoic/silaform amides,[27,28] or also radicaloids[29] (Scheme 1). Such species are highly sensitive and a skilled handling of such compounds is required as the reactivity is substantially different to that of organic counterparts. The problem with obtaining inorganic crown ethers imitating the organic counterpart, however, is probably ascribed to the specific Si–O bond character.

This is to date controversially discussed and regards siloxane donors as poorly coordinating. Various explanations in literature conclude a lower basicity of Si–O–Si groups compared to C–O–C groups which made silicon-based ligands unattractive for their use in coordination chemistry: Negative hyperconjugation interactions of $n_O \rightarrow \sigma^*_{Si-C}$ type are predominantly discussed.[30–33] When siloxanes coordinate Lewis acids, this $n_O \rightarrow \sigma^*_{Si-C}$ interaction competes with the $n_O \rightarrow M^{n+}$ interaction. Due to the described orbital overlaps, covalency is responsible for the low basicity. On the other hand, the Si–O bond is much more polarized and thus ionic compared to ethers. However, the oxygen atoms do not readily provide electron density for metal bonding. Electron density around oxygen is spatially delocalized,[34] and met-

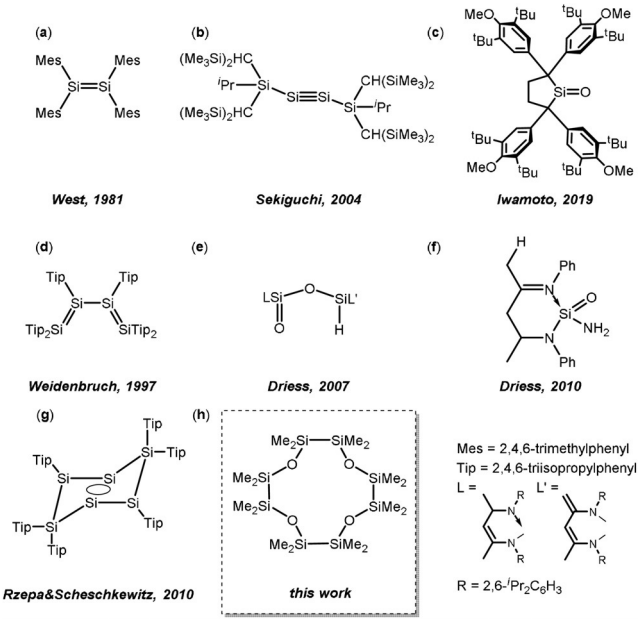

Scheme 1. Advances in a silicon chemistry imitating important organic compounds: a) alkene→disilene,[16] b) alkyne→disilyne,[17] c) ketone→silanone,[23] d) diene→siladiene,[19] e) ester→silanoic ester,[24] f) amide→silanoic amide,[27] g) benzene→hexasilabenzene,[18] h) [12]crown-4 (cyclic polyether)→octasila[12]crown-4 (cyclic sila-polyether).

[*] Dr. F. Dankert, R.-M. Richter, Prof. Dr. F. Weigend, Dr. X. Xie, Dr. M. Balmer, Prof. Dr. C. von Hänisch
Fachbereich Chemie, Philipps-Universität Marburg
Hans-Meerwein-Strasse 4, 35032 Marburg (Germany)
E-mail: florian.weigend@staff.uni-marburg.de
carsten.vonhaenisch@staff.uni-marburg.de

Supporting information and the ORCID identification number(s) for the author(s) of this article can be found under: https://doi.org/10.1002/anie.202014822.

$al^{+}\cdots Si^{\delta+}$ repulsive interactions disrupt metal binding.[35,36] Covalency and ionicity were for long time opposed to each other but, according to quantum chemical calculations, have about the same importance as both increase simultaneously when approaching larger Si-O-Si angles.[37] As mentioned, Si–O donors are described as weakly coordinating and thus coordination compounds of neutral siloxane ligands were mostly obtained using highly reactive compounds or WCAs such as perfluorinated alkoxy aluminates (WCA = weakly coordinating anion).[35,38–43] However, the understanding of siloxane ligands has crucially moved on in the past few years. As several works show, early group one and especially group two ions can be effectively bound within siloxane moieties and the nature of the cation has to be considered when siloxanes are used for silyl-ether coordination.[44–48] Another key factor for comparing organic (crown) ethers with siloxane ligands is the architecture of the ligand moiety. Most silicon-based ligands are constructed out of $-OSiMe_2-$ units rather than $-OC_2H_4-$ units. This structural difference leads to increased ring strain upon coordination.[49,50] For a few years we therefore investigated the coordination ability of sila-(crown) ethers with one, two, or three $-Si_2Me_4-$ units as well as C_2H_4 groups between oxygen atoms.[51–58] We could demonstrate that these hybrid ligands coordinate well and the cooperative effects of siloxane-oxygen donors as well as etheric oxygen donors yield stable complexes.[51–58] To date, however, exclusively silicon-based crown-ether analogs of ^2D_n type ($^2D_n = (Si_2Me_4O)_n$) were unavailable.

Herein, we report on exclusively disilanyl-bearing cyclosiloxanes and their metal complexes which are available by s-block-metal templated Si–O bond activation. NMR spectroscopic investigations, single-crystal X-ray diffraction experiments, as well as quantum chemical calculations were carried out to impart an understanding of these—to the best of our knowledge—first-ever characterized (metal) complexes of silicon-based crown-ether analogues of ^2D_n type.

Results and Discussion

Synthesis and Structure

Cyclic ligands containing siloxane moieties can be ring-opened and also deconstructed by either strong acids, various organometallic bases or suitable metal–anion combinations.[58–61] ROP (ROP = ring-opening polymerization) of cyclic silaethers, however, is a challenge as organometallic bases can initiate Si–Si bond cleavage and cationic ROP requires very strong acids such as triflic acid.[59] As we demonstrate herein, a milder approach turned out to be expedient for the synthesis of inorganic crown ethers. Combining the small WCA $[GaI_4]^-$, a chemically rather hard metal cation, and a suitable sila-precursor was identified as the method of choice. A suitable sila-precursor for oligomerization is $^2D_2$ (**I**). The proton affinity and the basicity of **I** are described to be significantly higher than those of siloxanes of the D_n type, including very reactive D_3.[62,63] For this reason, we started investigating $^2D_2$/s-block metal iodide/gallium(III) iodide systems and used LiI at first (Scheme 2). Indeed, an oligomerization of the cyclic ligand occurs from the reaction

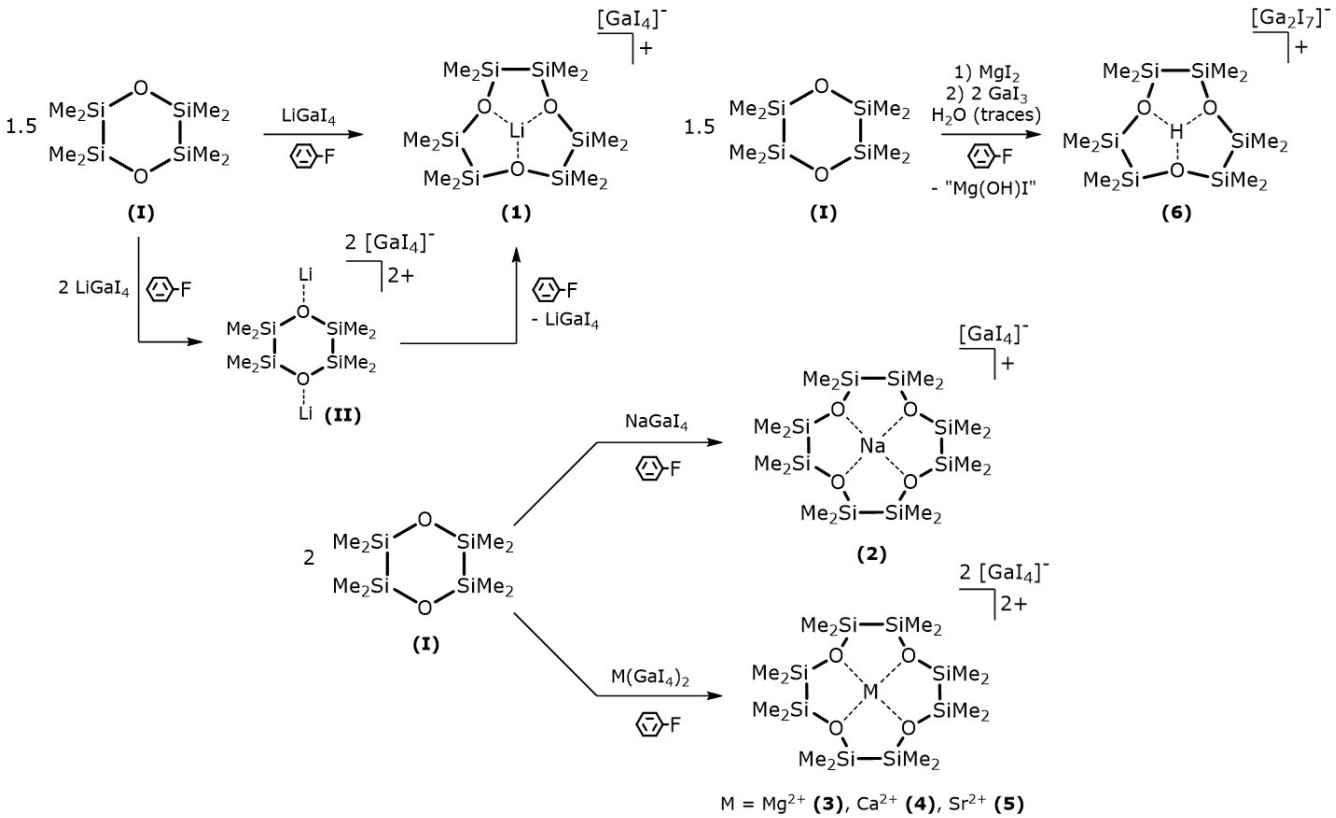

Scheme 2. Formation of inorganic crown-ether complexes of the s-block elements. For experimental details see SI.

of LiI with GaI_3 and $^2D_2$. However, the outcome of the reaction highly depends on the reaction time and stoichiometry of the metal salt. Upon stirring 1.0 equiv of in situ generated $LiGaI_4$ and 1.5 equiv **I** for 2 h at 70 °C in Ph–F, we observed formation of $[Li_2(^2D_2)(GaI_4)_2]$ (**II**), which shows two Li^+ ions coordinated by one $^2D_2$ ligand and $[GaI_4]^-$ counterions (Figure 1 and S2). According to single-crystal X-ray diffraction analysis, a one-dimensional coordination polymer is obtained (see Figure S2). The stoichiometry of the reaction protocol does not fit for this compound, but the reaction is finely reproducible under these conditions with an average yield of 80 % based on the used $LiGaI_4$. The ^{29}Si NMR spectrum of a freshly prepared sample of **II** in CD_2Cl_2 shows a resonance at 8.0 ppm for **II**, a signal of the new complex **1** (see below) and small resonances of unknown decomposition products (see SI). Comparing the observed resonance of **II** with that found for **I** [$\delta(^{29}Si) = 3.6$ ppm] supports the interaction of **I** with Li^+ in solution. Coordination of **I** to Li^+ causes a significant change in the bonding situation of the Si–O linkage. For **II**, the Si-O-Si angles are smaller and the Si–O bonds are longer than for **I**, as can be seen from the crystal structures of **I** and **II** (Figure 1). From this respective intermediate product, we concluded that ring opening requires effective Si–O bond activation and we repeated the reaction procedure with 2.0 equiv of $LiGaI_4$ and longer reaction times. Stirring **I** and $LiGaI_4$ or isolated **II** in Ph–F overnight at 70 °C selectively yields the compound $[Li(^2D_3)GaI_4]$ (**1**) ($^2D_3 = (Me_4Si_2O)_3$ = 1,2,4,5,7,8-hexasila-[9]crown-3) in 54 % yield based on $^2D_2$. In this compound the silicon-based crown ether $^2D_3$ is threefold coordinating the lithium ion (Figure 2, left) and the ^{29}Si NMR spectrum in CD_2Cl_2 solution shows a resonance at lower field (15.5 ppm) which compares very well with the hybrid crown compound [Li(1,2,4,5-tetrasila[12]crown-4)OTf] where a single resonance is observed at 15.9 ppm for the inner Si-atoms.[52]

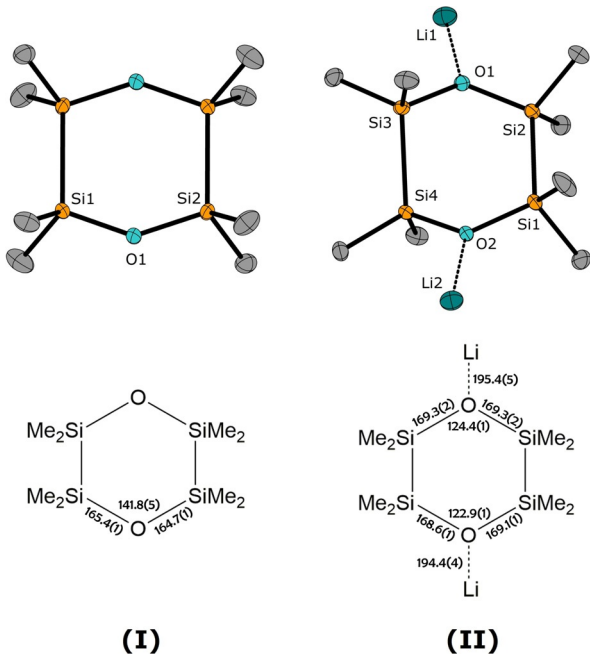

Figure 1. Structural comparison of the molecular structures of **I** and **II** in the crystal.[86] Thermal displacement ellipsoids represent the 50 % probability level. Half a molecule of **I** is symmetry-generated over 1−*x*, 1−*y*, 1−*z*. Hydrogen atoms as well as attached $[GaI_4]^-$ anions of **II** are omitted for clarity. Bond lengths are depicted in [pm] and angles in [°].

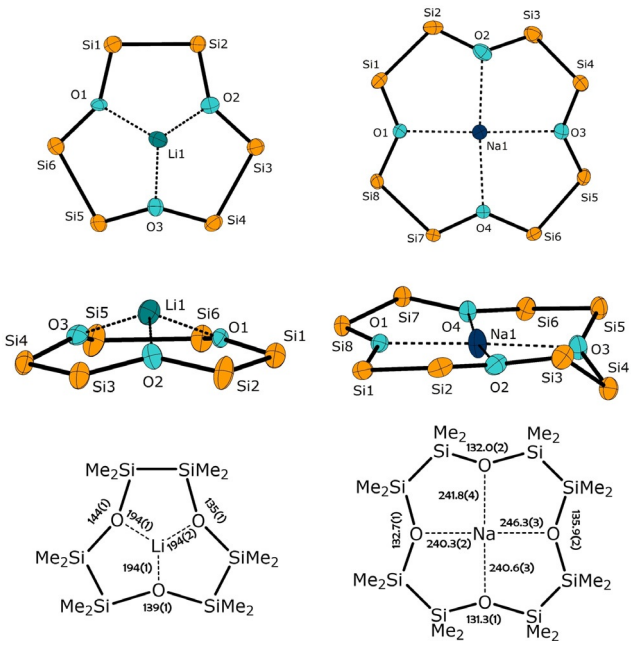

Figure 2. Comparison of the geometric features of alkali metal complexes of inorganic crown ethers.[86] The molecular structures of **1** (left) and **2** (right) in the crystal are reduced to the inorganic skeleton. Anions as well as disordered parts are omitted for clarity. Thermal displacement ellipsoids represent the 50 % probability level. Atom distances are depicted in [pm] and angles in [°].

[9]Crown-3, the smallest member of the crown-ether family, is barely used for coordination chemistry. The Li^+ ion in $[Li(naphtho[9]crown\text{-}3)_2]ClO_4$ is located 139.5 pm above the spanned plane of the three oxygen atoms.[64] In **1**, the Li^+ ion is much more sunken into the cavity of the ligand as it is in this case 69.2 pm above the spanned plane of the oxygen atoms. Due to a lower coordination number at Li^+, the O–Li atom distances are slightly smaller than, for example, in $[Li(D_6)Al_F]$ ($Al_F = [Al\{OC(CF_3)_3\}_4]^-$) (194(1) –194(2) pm in **1** and 201(1) –208(1) pm in the D_6 complex). The Si-O-Si angles of **1** vary from 135(1) to 144(1)°. Thus, the ligands' architecture in the complex bears Si-O-Si angles comparable with those in the mentioned D_6 complex where Si-$O_{coord.}$-Si angles of 139.5(4)–141.6(4)° are present. As can be seen from both structures **II** and **1**, the siloxane coordination highly depends on the reaction conditions with exocyclic metal coordination as a crucial step due to Si–O bond activation. Metal templation then enables a higher number of silyl–ether contacts. To obtain a larger crown ether $^2D_2$ was reacted with sodium iodide as well as GaI_3. Indeed the larger silicon-based crown ether $^2D_4$ ($^2D_4 = (Me_4Si_2O)_4$ = 1,2,4,5,7,8,10,11-octasila[12]crown-4) is formed (Figure 2, right). The solid-state structure of $[Na(^2D_4)GaI_4]$ (**2**) shows a sodium ion bound by all of the crown ethers oxygen atoms. The larger cavity of the twelve-membered cycle can accommodate the sodium ion in a square-planar fashion ($r_i[Na^+]_{CN5} = 100$ pm)[65] as the oxygen mean plane···Na^+ distance measures only 5 pm.

The Si-O-Si angles in **2** measure 131.3(1) to 135.9(2)°, which compares well with the Si-O-Si angle in [Na(1,2,4,5-tetrasila-benzo[15]crown-5)I].[44] In solution, the ^{29}Si NMR resonance is observed at 13.1 ppm in deuterated dichloromethane and reveals ligand–metal interaction to be also present in solution.

We also employed the in situ generated, higher homologous alkali-metal salts $MGaI_4$ ($M = K^+$-Cs^+) but attempts at isolating corresponding crown-ether complexes failed so far. This is probably due to the nature of the respective cations which are chemically too soft and are not polarising the Si–O bond properly for oligomerization. For this reason, we also employed the chemically harder alkaline earth metals for the synthesis of such inorganic crown ethers. The alkali-metal ions Mg^{2+}–Sr^{2+} turned out to be suitable templates yielding $[M(^2D_4)(GaI_4)_2]$ ($M = Mg^{2+}$ (**3**), Ca^{2+} (**4**), Sr^{2+} (**5**)) but crystal structures could only be obtained for **4** and **5**. Salts of Be^{2+} and Ba^{2+} had also been reacted with **I**. Whereas beryllium halides form literature-related[57] polyolate complexes which will be published in due course, $Ba(GaI_4)_2$ shows no reactivity towards $^2D_2$. As also observed in **2**, the metal ion in compound **4** is situated in plane with the ligand but the Si-O-Si angles are smaller in comparison to **2** (131.3(1) to 135.9(2)° in **2** and 126.9 to 127.9° in **4**). The O–Ca bonds are 237.0(6) and 239.7(9) pm long (Figure 3, left). Silyl ether bonding of this silicon-based macrocycle is stronger towards the group 2 metal and the ligand shows an enhanced basicity even though there are now two metal–anion interactions which are known to perturb silyl ether coordination.[40] These values compare well with the atom distances as well as Si-O-Si angle found in the hybrid crown-ether complex [Ca(1,2,4,5-tetrasila-benzo-[15]crown-5)I_2].[44] In solution, a distinct low-field shifted resonance of 19.2 ppm is observed in the ^{29}Si NMR experiment, which proves the strong coordination of the ligand in solution. Interestingly, and in contrast to all other herein characterized compounds, **4** is stable towards moisture as $[Ca(^2D_4)(GaClI_3)_2]$ (**4a**) crystallizes in an NMR tube from CD_2Cl_2 solution exposed to moisture (see Figure S11). The ligand moiety is maintained under air and the metal center remains inside the cavity. The crystal structure determination of the Sr^{2+} species **5** was a challenge. The compound reveals an intrinsic disorder problem and the only suitable crystals for SC-XRD could be grown from a Ph–F solution. We were still able to determine the molecular structure but have in this case used a completely restrained model to fix the refinement with $P2_12_12_1$ as the most suitable space group (Figures S6 and S9). In solution, the respective singlet of **5** in ^{29}Si NMR spectroscopy is observed at 16.6 ppm proving strong interactions of the Si–O moiety with Sr^{2+}.

As mentioned above, no crystal structure could be obtained for compound **3**. This is most likely due to the very high sensitivity of the compound. **3** can only be obtained using MgI_2 with a purity of 99.996 % (denoted as "ultra dry"). We could detect several decomposition products (see compounds **S1** and **S2**) while attempting to determine the crystal structure of **3**. However, one compound was obtained which aroused our interest. We were able to obtain and characterize a compound of a proton in $^2D_3$. $[H(^2D_3)][Ga_2I_7]$ (**6**) was obtained after contaminating a Ph–F solution of **3** with immersion oil, which is often used for preparing single crystals. The compound could be reproduced employing different reaction conditions (see SI). We assume that the formation of the Lewis-acid system GaI_3/MgI_2 and probably also the high lattice energy of $Mg(OH)_2$ facilitate the formation of a proton–siloxane complex when traces of H_2O are present. The field of proton complexes has been reviewed by Chambron and Meyer[66] but as outlined, proton complexes are limited to organic-type ligands. Most of them resemble crown ether- or cryptand-like macrocycles. A handful of open-chained complexes are also characterized[67–69] but compound **6** is the very first example of proton coordination within a cyclic siloxane. Crystals of **6** generally exhibit a high quality so that it was possible to determine the molecular structure precisely. The encircled proton was located and refined as an independent isotropic atom in the middle of the crown-ether moiety. Due to oscillation of the refined hydrogen atom, very soft SADI (SADI = same atomic distance) restraints were employed, though. There are related compounds published in literature, such as protonated organic crown-ether and cryptand compounds,[66] diverse silanols,[70] and silanolates.[71] Protonated siloxane linkages, though, are overall very rare. To the best of our knowledge, there are only two structurally characterized disiloxonium-ions, one from Sekiguchi[72] and the other one from Müller.[73] Even though the Brønsted acid/base chemistry is not exactly part of our study we want to emphasize that compound **6** might be interesting in a context of proton chelators. Siloxanes prove to be an interesting new possibility to

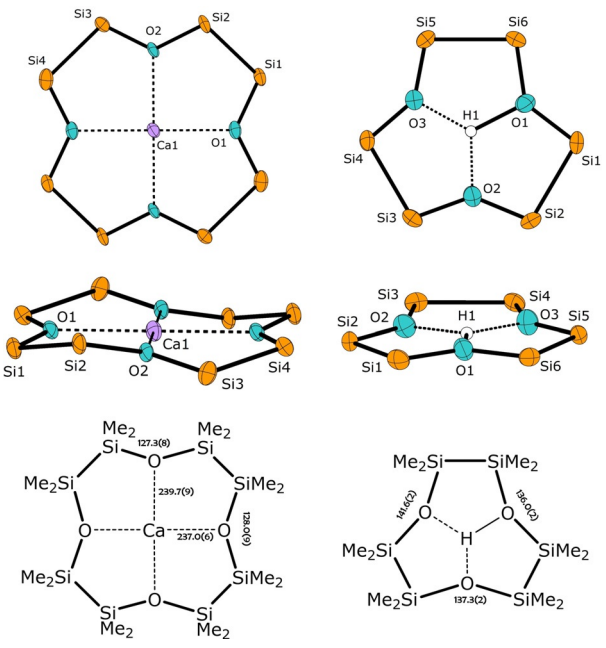

Figure 3. The geometric features of an alkaline earth metal and proton complex of an inorganic crown ether.[86] The molecular structures of **4** (left) and **6** (right) in the crystal are reduced to the inorganic skeleton. Anions as well as disordered parts are omitted for clarity. Thermal displacement ellipsoids represent the 50% probability level. Non-labeled atoms are symmetry-generated over $1-x$, $1-y$, $1-z$. Atom distances are depicted in [pm] and angles in [°].

establish such a chemistry, even though siloxanes were long assumed to be not very basic at all.

As the metal complexes described above, compound **6** shows a strong low-field shifted signal compared to the starting compound **I** in the ^{29}Si NMR spectrum at 21.2 ppm. In the ^{1}H NMR spectrum of **6**, a major signal at 0.52 ppm was observed, which was readily assigned to the protons of the methyl groups. In addition, two broad signals at 7.89 and 9.38 ppm were observed. An integral of these signals revealed relative intensities of 36:0.8:0.5. We propose these two broad signals to be due to the trapped proton. The observation of twin resonance signals was also reported for protons trapped in crown ethers.[74] Our efforts to obtain long-range correlation and exchange spectroscopy failed. We observed the disappearance of these two signals together with the major signal about 3 hours after sample preparation, indicating that compound **6** in solution is not stable over long periods of time.

Table 1: NMR Chemical Shifts and diffusion coefficients in CD_2Cl_2 at 298 K.

compound		^{1}H [ppm]	^{13}C [ppm]	^{29}Si [ppm]	D^{exp} [10^{-9} m^2 s^{-1}]	$r_{exp.}$ [Å][a]	r_{calcd} [Å]
$^{2}D_2$ (**I**)		0.20	2.6	3.6	1.53	3.5	3.5[b]
$[Li_2(^{2}D_2)]^{2+}$	(cation of **II**)	0.36	2.7	8.0	1.21	4.4	4.3[b]
$[Li(^{2}D_3)]^{+}$	(cation of **1**)	0.47	3.1	15.5	1.03	5.1	4.7[b]
$[Na(^{2}D_4)]^{+}$	(cation of **2**)	0.45	2.9	13.1	0.99	6.0	5.2[b]
$[Mg(^{2}D_4)]^{2+}$	(cation of **3**)	0.71	3.5	25.7	0.87	6.1	n.d.[c]
$[Ca(^{2}D_4)]^{2+}$	(cation of **4**)	0.47	4.0	19.2	0.87	6.1	5.6[d]
$[Sr(^{2}D_4)]^{2+}$	(cation of **5**)	0.64	4.4	16.6	0.86	6.1	5.2[d]
$[H(^{2}D_3)]^{+}$	(cation of **6**)	0.52	1.7	21.2	1.09	4.9	4.4[d]

[a] Hydrodynamic radius based on the experimental diffusion coefficients measured in CD_2Cl_2 at 298 K and Stoke–Einstein equation $D = k_B T/6\pi\eta r$. [b] Radius calculated from molecular hard-sphere volume increments.[79] [c] Not determined. [d] Radius estimated from X-ray.

NMR Spectroscopic Investigations

Due to the fact that solid-state structures are not necessarily maintained in solution, especially when molecules have a high tendency to form oligomers,[75] further investigations are necessary to proof the existence of the respective ligand moiety in solution. By taking advantage of the pulsed-field gradient (PFG), diffusion-ordered spectroscopy (DOSY) experiments provide diffusion coefficients of molecules in solution. In related works, PFG diffusion experiments proved to be powerful in the study of various aggregates in solution.[75,76] According to the Stoke–Einstein equation the size of the molecules can be determined. Stejskal–Tanner plots are used to display the diffusion behavior of molecules in solution, whereby the attenuation of signal intensities in response to the applied gradient strength is plotted in logarithmic scale.[77,78]

Therefore, the slope of the Stejskal–Tanner plot corresponds directly to the diffusion coefficient of the molecule. For example, an overlay of the Stejskal–Tanner plots of the solvent CD_2Cl_2, $^{2}D_2$ (**I**), the Li^+ complex of a nine-membered macrocycle $[Li(^{2}D_3)]^{+}$ (cation of **1**), and the sodium complex of a twelve-membered macrocycle $[Na(^{2}D_4)]^{+}$ (cation of **2**) is shown in Figure S51, which clearly demonstrates the correlation of ligand size with the cation incorporated. The obtained diffusion coefficients for all characterized compounds and the molecular radii are summarized in Table 1. The obtained molecular radii agree well with those of the molecules in solid state.

The combination of the observed chemical shifts and the determined ion radius verified that the cations $[Li_2(^{2}D_2)]^{2+}$ and $[Li(^{2}D_3)]^{+}$ bear a six- and nine-membered (macro-)cyclic ligand in solution, while $[Na(^{2}D_4)]^{+}$, $[Mg(^{2}D_4)]^{2+}$, $[Ca(^{2}D_4)]^{2+}$, and $[Sr(^{2}D_4)]^{2+}$ all bear a twelve-membered macrocyclic ligand in solution.

Extraction of Unoccupied $^{2}D_n$ Ligands

A remaining question at this point is if the cation which is used for the template synthesis can be removed from the ligands to obtain a free ligand species. For this purpose, we have chosen compound **4** as it shows the highest stability and can be synthesized in high yields. After isolating crystalline **4**, the crystals were dissolved in the donor solvent MeCN. It could be observed by means of ^{1}H NMR spectroscopy that the metal ion is indeed readily displaced in favor of MeCN coordination. Adding *n*-pentane to a MeCN/$[Ca(^{2}D_4)(GaI_4)_2]$ solution results in the formation of two separate phases. The sila-ligands can therefore be extracted from the mixture by separating the *n*-pentane solution from MeCN. After workup, an oily residue is obtained from the *n*-pentane phase. NMR spectroscopy revealed that the oil contained several species indicating that free ligand $^{2}D_4$ is not stable without a template. The ^{1}H NMR spectrum (CD_2Cl_2, 300 MHz, 298 K) shows overlapping resonances at 0.16, 0.17, and 0.20 ppm. These peaks can be tentatively assigned to $^{2}D_4$ (**7**, 0.16 ppm), $^{2}D_5$ (**8**, 0.17 ppm), and $^{2}D_2$ (**I**, 0.20 ppm). This assignment is supported by ^{1}H-^{29}Si HMBC, ^{1}H-^{13}C HMQC experiments and by LIFDI$^+$MS (LIFDI = liquid injection field desorption ionization; MS = mass spectrometry) studies (Scheme 3). The main product of a freshly prepared $^{2}D_n$ mixture according to the LIFDI$^+$MS is $^{2}D_4$ (relative abundance of 100%, *m*/*z* calcd 528.17067; found 528.17196), and thus the ^{1}H NMR main peak at 0.16 ppm and the correlating peaks from ^{13}C and ^{29}Si NMR are assigned to $^{2}D_4$ (^{13}C NMR: 2.38 ppm, ^{29}Si NMR: 0.4 ppm). $^{2}D_5$ (relative abundance of 30%, *m*/*z* calcd 660.21334; found 660.21494) is therefore assigned to the ^{1}H NMR peak of 0.17 ppm and its respective correlations (^{13}C NMR: 2.35 ppm, ^{29}Si NMR: 0.9 ppm). The peak at 0.20 ppm and the respective correlations (^{13}C NMR: 2.36 ppm, ^{29}Si NMR: 3.4 ppm) could be assigned to **I** as we were using this as our well-known starting material.[80] LIFDI$^+$MS further suggests the existence of $^{2}D_6$ (**9**) in traces (relative abundance of 8%, *m*/*z* calcd 792.25601; found 792.25693). Is the oil considered as a mixture of $(Me_4Si_2O)_n$ (n = 2–6), the turnover to free ligand species is quantitative,

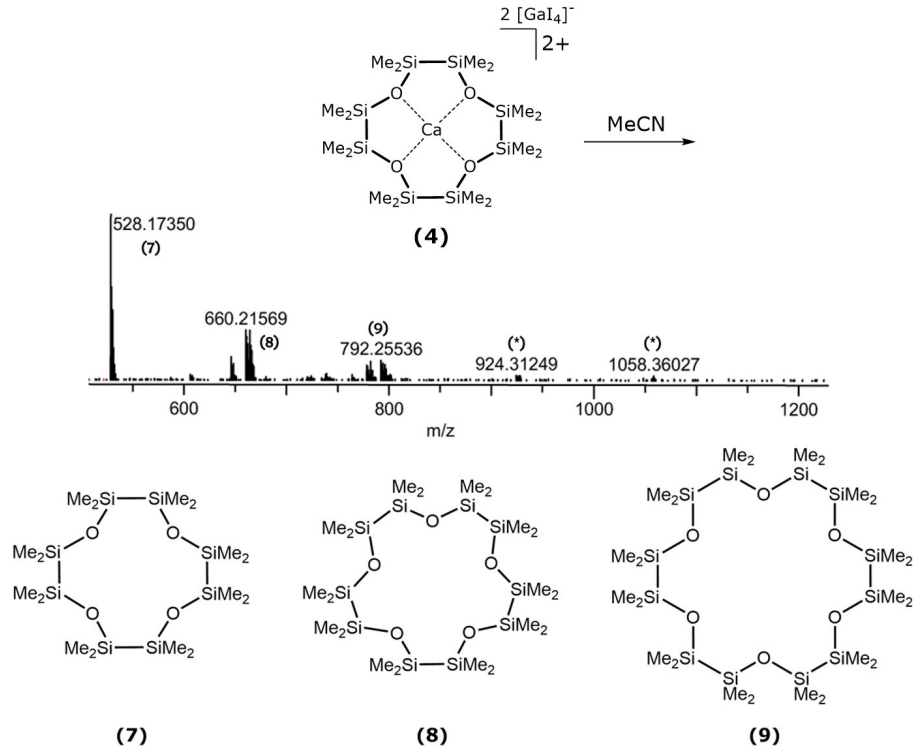

Scheme 3. LIFDI(+) MS spectrum of a ^2D_n mixture after conversion of compound **4** with MeCN. Compounds **7**–**9** were detected as positively charged radical species. For the respective HR-MS spectra, please see the SI. The *m/z* relations marked with asterisk (*) can tentatively be assigned to even higher oligomers of $^2D_2$ such as $^2D_7$ and $^2D_8$, but no suitable HR-MS was obtained due to poor signal-to-noise ratio.

which is evident from NMR spectroscopy as coordinated species are no longer found upon MeCN addition. In solution, free ligand species are not stable. As $^2D_4$ is the main product right after the extraction, the integral of **I** increases with time. After nine weeks exclusively **I** is found to be present. Hence, we observe a reversible reaction behavior here. We assume this back-reaction is entropically driven and may be catalyzed by traces of metal cations and especially by $I^-/[GaI_4]^-$ anions as quantum chemical calculation of the reaction of $^2D_2 + {}^2D_2 \rightarrow {}^2D_4$ is enthalpically insignificant (see next section).

Quantum Chemical Calculations

Quantum chemical calculations[81] (PBE functional,[82] TZVP bases[83]) were carried out to estimate the ability of the different ^2D_n-type species to coordinate M^{x+} ions, also relative to D_n-type ($D = SiMe_2O$) species as well as to organic crown ethers. Further, they were done to shed light on the formation of larger rings from $^2D_2$, in particular on the role of M^{x+} and I^-, $[GaI_4]^-$ for this process. The first issue was tackled by the calculation of energies for exchange reactions according to Equation (1)].

$$[M(L_2)X_n]^{(1-n)+} + L_1 \rightarrow [M(L_1)X_n]^{(1-n)+} + L_2 \quad (1)$$

These energies directly allow a comparison of the affinity of L_1 and L_2 for a metal ion M^+ in the absence ($n = 0$) or the presence ($n = 1$) of $X^- = I^-$, $[GaI_4]^-$. The calculations were done for reactions in the gas phase as well as in solvents with a dielectric constant $\varepsilon = 6$ (oriented at Ph–F) within the conductor-like screening model (COSMO[84]). Results comparing $^2D_3$, $^2D_4$ for M = Li, Na are exemplarily shown in Table 2. In case of M = Li, the explicit consideration of at least X = I is required to correctly reproduce the preference of $^2D_3$ over $^2D_4$; for X = $[GaI_4]$ results do not change significantly. In contrast, for M = Na the experimentally observed preference of $^2D_4$ for Na is correctly reproduced for all models. Moreover, when employing COSMO, then values with and without additional explicit consideration of the anion are similar (last line in Table 2), indicating that for a comparison of ligand affinities the employment of COSMO without explicit consideration of anions is sufficient. For this model and M = Na energies comparing $^2D_2$, $^2D_3$, $^2D_4$, D_5, D_6, as well as for the crown ethers [3*n*]-crown-*n* (C_n), $n = 4$, 5, 6 according to Equation (1) are listed in the Table 3. For Na, $^2D_4$ is more attractive than most of the other ligands (exceptions are the two largest crown ethers).

The overall most attractive ligand is [18]crown-6, and the least attractive is $^2D_2$, for which Na resides outside the ring. A

Table 2: Reaction energies according to Equation (1) for $L_1 = {}^2D_4$, $L_2 = {}^2D_3$ in kJ mol^{-1}. Negative values indicate a preference for $^2D_4$ to bind Na^+/Li^+ in the gas phase ($\varepsilon = 1$) or in a solvent with $\varepsilon = 6$.

	$n = 0$	$n = 1$, X = I^-	$n = 1$, X = $[GaI_4]^-$
Li, $\varepsilon = 1$	−35	18	24
Li, $\varepsilon = 6$	−17	21	21
Na, $\varepsilon = 1$	−65	−32	−5
Na, $\varepsilon = 6$	−35	−23	−20

Table 3: Energies for reactions $[Na(L_2)]^+ + L_1 \rightarrow [Na(L_1)]^+ + L_2$ in kJ mol^{-1} for $\varepsilon = 6$. The rows refer to L_1 and the columns to L_2. (L_1, $L_2 = {}^2D_2$, $^2D_3$, $^2D_4$, D_5, D_6, C_4, C_5, C_6; C_n is an abbreviation for [3*n*]crown-*n*). For instance, the energy for the reaction $[Na(^2D_3)]^+ + {}^2D_4 \rightarrow [Na(^2D_4)]^+ + {}^2D_3$, which amounts to −35 kJ mol^{-1}, is found in the row labeled $^2D_4$ and the column labeled $^2D_3$.

	$^2D_2$	$^2D_3$	$^2D_4$	D_5	D_6	C_4	C_5	C_6
$^2D_2$	0	26	61	38	60	51	75	107
$^2D_3$	−26	0	35	12	33	25	49	81
$^2D_4$	−61	−35	0	−23	−2	−10	14	46
D_5	−38	−12	23	0	21	13	37	69
D_6	−60	−33	2	−21	0	−8	15	47
C_4	−51	−25	10	−13	8	0	24	56
C_5	−75	−49	−14	−37	−15	−24	0	32
C_6	−107	−81	−46	−69	−47	−56	−32	0

rough estimation for the sequence of affinity may be obtained by forming the sum over a line or column of Table 3, yielding (with decreasing affinity):

$$C_6 > C_5 > {}^2D_4 \approx D_6 > C_4 > D_5 > {}^2D_3 > {}^2D_2$$

Thermal contributions to the free enthalpy obtained within the harmonic oscillator rigid rotor model at room temperature are rather small. They were exemplarily calculated for M = Na and L_1, $L_2 = {}^2D_3$, $^2D_4$, for which they amount to 7 kJ mol^{-1} (in favor of the left-hand side, $[Na(^2D_4)]^+ + {}^2D_3$).

The formation of larger rings from smaller ones was investigated exemplarily for $^2D_4$ formed from two $^2D_2$ rings. The energy gain for the (hypothetic) reaction $^2D_2 + {}^2D_2 \rightarrow {}^2D_4$ is insignificant, −4 kJ mol^{-1}. Matters are different as soon as M^{x+} such as Na^+ is present. The energy of the corresponding reaction, $[Na(^2D_2)]^+ + {}^2D_2 \rightarrow [Na(^2D_4)]^+$, amounts to −148 kJ mol^{-1} for $\varepsilon = 1$, and still −51 kJ mol^{-1} for $\varepsilon = 6$. So, the presence of Na^+ obviously is important for the reaction. Nevertheless, a significant energy barrier may be expected. Reaction pathways were identified and pre-optimized with a nudge-band-type method proposed by Plessow,[85] followed by the optimization of the extrema. For technical reasons all kinds of structure optimizations were done for $\varepsilon = 1$, followed by single-point energy calculations with $\varepsilon = 6$. The error of this approximation was estimated for several structures along the path and turned out to be 5 kJ mol^{-1} at most, which is much less than the influence of COSMO itself, see below. Details of the optimization and of the optimized structures are specified in the Supporting Information. The energy profile for the formation of $[Na(^2D_4)]^+$ is shown in Figure 4. The formation of an intermediate complex $[(^2D_2)Na(^2D_2)]^+$ from two $^2D_2$ rings and Na^+ (via $[Na(^2D_2)]^+ + {}^2D_2$) comes with an energy gain of 36 kJ mol^{-1}, without any significant barrier. For the pathway from this complex to $[Na(^2D_4)]^+$ we find a single transition state (TS1), which is higher in energy than the initial state by 297 kJ mol^{-1}. One may conclude that this barrier prohibits the transformation. Further, from inspection of the structure of TS1, see Figure 4, it is evident that Na is only weakly involved in the transition, which also probably rules out the transformation of two bare $^2D_2$ rings to $^2D_4$ (or back). Again, considering thermal contributions to the free enthalpy change the situation by less than 6 kJ mol^{-1}.

For the additional presence of I^- (which appears to be a reasonable model for $[GaI_4]^-$, see above), matters are

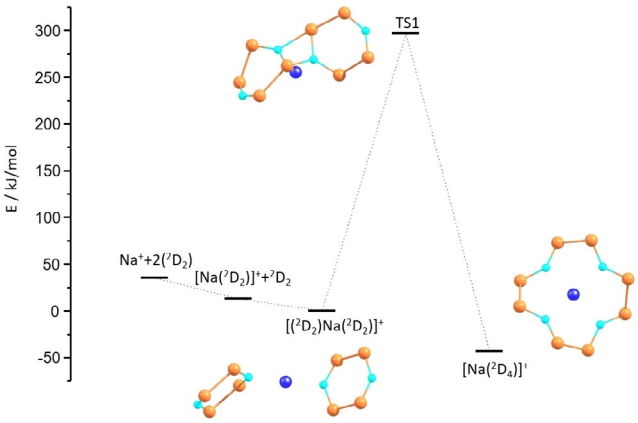

Figure 4. Energy profile for the pathway from $Na^+ + 2\,{}^2D_2$ via $[(^2D_2)Na(^2D_2)]^+$ to $[Na(^2D_4)]^+$. Silicon: orange, oxygen: light blue, sodium: blue, iodine: red.

different, see Figure 5. Starting form $2\,{}^2D_2 + Na^+ + I^-$ the intermediate complex $[(^2D_2)NaI(^2D_2)]$ is obtained without barriers; the energy gain is 149 kJ mol^{-1}. For the transition from this complex to $[Na(^2D_4)I]$ (lower in energy by 43 kJ mol^{-1}) we find three transition states and two intermediate local minima (TS1, LM1, TS2, LM2, TS3), which are higher in energy than $^2D_2NaI^2D_2$ by 133–192 kJ mol^{-1}, but thus in the same range as the initial state, $2\,{}^2D_2 + Na^+ + I^-$, as well as the final state, $[Na(^2D_4)]^+ + I^-$, which is higher in energy than $[Na(^2D_4)I]$ by 91 kJ mol^{-1}. It needs to be said that the energies of the first step and the last step strongly depend on the choice of ε, as (atomic) ions—in particular I^-—are involved here; for instance, for the extreme case $\varepsilon = \infty$ they amount to 8 and 14 kJ mol^{-1} (instead of 149 and 91 kJ mol^{-1} for $\varepsilon = 6$). Nevertheless, overall the reaction is more likely to happen in presence of I^- than in its absence. In detail, the

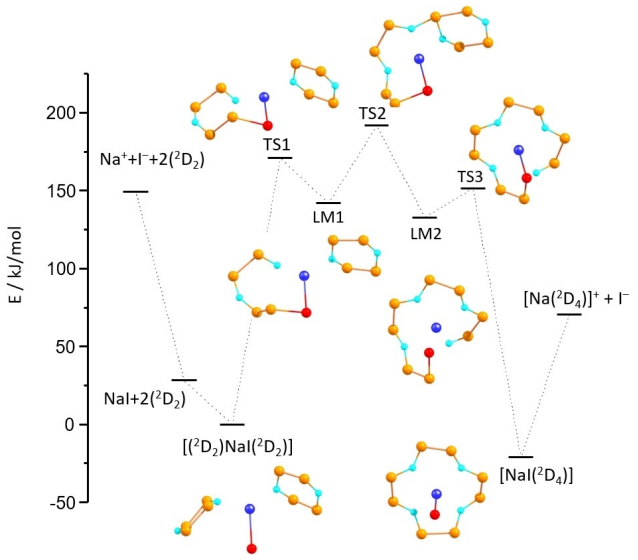

Figure 5. Energy profile for the pathway from $Na^+ + I^- + 2\,{}^2D_2$ via $[(^2D_2)NaI(^2D_2)]$ and $[Na(^2D_4)I]$ to $[Na(^2D_4)]^+ + I^-$. Carbon and hydrogen atoms are omitted for clarity. Silicon: orange, oxygen: light blue, sodium: blue, iodine: red.

I^- ion approaches an Si atom of the left $^2D_2$ unit, which simultaneously opens the Si–O bond in this ring (TS1). Next, the dangling O atom approaches an Si atom of the right $^2D_2$ unit, which, after slight rearrangement of the Me groups (TS2), enables the formation of a bond between the two units and simultaneously opens one Si–O bond in the second ring (LM2). The barrier when forming the second bond between the units (TS3) is low. Overall, the calculations show that it is the presence of I^- that facilitates the reaction from $2\,^2D_2 + Na^+$ to $[Na(^2D_4)]^+$ by nucleophilic assistance. As Na^+ is not much involved in the mechanism, one might assume that a similar assistance is the reason for the oligomerization of the metal ion-free $^2D_4$ ring.

Conclusion

By this combined experimental and theoretical study, we were able to show that siloxane units can be efficiently activated by a combination of hard cations and iodide/tetraiodidogallate counterions. In this way, silicon analogues of the crown ethers could be prepared for the first time and investigated on the basis of their complexes with different cations. Thus, we have added another piece of the puzzle of replicating functional organic molecules with silicon.

Acknowledgements

This work was financially supported by the Deutsche Forschungsgemeinschaft (DFG, HA 3466/8-3). Open access funding enabled and organized by Projekt DEAL.

Conflict of interest

The authors declare no conflict of interest.

Keywords: host–guest systems · inorganic crown ethers · ion recognition · reaction mechanism · templates

[1] G. W. Gokel, W. M. Leevy, M. E. Weber, *Chem. Rev.* **2004**, *104*, 2723 – 2750.
[2] A. Swidan, C. L. B. Macdonald, *Chem. Soc. Rev.* **2016**, *45*, 3883 – 3915.
[3] J. W. Steed, *Coord. Chem. Rev.* **2001**, *215*, 171 – 221.
[4] C. J. Pedersen, *J. Am. Chem. Soc.* **1967**, *89*, 7017 – 7036.
[5] C. J. Pedersen, *Angew. Chem. Int. Ed. Engl.* **1988**, *27*, 1021 – 1027; *Angew. Chem.* **1988**, *100*, 1053 – 1059.
[6] T. Chivers, I. Manners, *Inorganic Rings and Polymers of the p-Block Elements: From Fundamentals to Applications*, Royal Society Of Chemistry, Cambridge, **2009**.
[7] W. Xuan, A. J. Surman, Q. Zheng, D.-L. Long, L. Cronin, *Angew. Chem. Int. Ed.* **2016**, *55*, 12703 – 12707; *Angew. Chem.* **2016**, *128*, 12895 – 12899.
[8] A. J. Plajer, R. García-Rodríguez, C. G. M. Benson, P. D. Matthews, A. D. Bond, S. Singh, L. H. Gade, D. S. Wright, *Angew. Chem. Int. Ed.* **2017**, *56*, 9087 – 9090; *Angew. Chem.* **2017**, *129*, 9215 – 9218.
[9] C. Donsbach, K. Reiter, D. Sundholm, F. Weigend, S. Dehnen, *Angew. Chem. Int. Ed.* **2018**, *57*, 8770 – 8774; *Angew. Chem.* **2018**, *130*, 8906 – 8910.
[10] S. G. Calera, D. S. Wright, *Dalton Trans.* **2010**, *39*, 5055 – 5065.
[11] A. Nordheider, T. Chivers, R. Thirumoorthi, I. Vargas-Baca, J. D. Woollins, *Chem. Commun.* **2012**, *48*, 6346 – 6348.
[12] M. Nishio, S. Inami, Y. Hayashi, *Eur. J. Inorg. Chem.* **2013**, 1876 – 1881.
[13] E. Block, E. V. Dikarev, R. S. Glass, J. Jin, B. Li, X. Li, S.-Z. Zhang, *J. Am. Chem. Soc.* **2006**, *128*, 14949 – 14961.
[14] A. J. Martínez-Martínez, D. R. Armstrong, B. Conway, B. J. Fleming, J. Klett, A. R. Kennedy, R. E. Mulvey, S. D. Robertson, C. T. O'Hara, *Chem. Sci.* **2014**, *5*, 771 – 781.
[15] B. Krebs, H.-U. Hürter, *Angew. Chem. Int. Ed. Engl.* **1980**, *19*, 481 – 482; *Angew. Chem.* **1980**, *92*, 479 – 480.
[16] R. West, M. J. Fink, J. Michl, *Science* **1981**, *214*, 1343 – 1344.
[17] A. Sekiguchi, R. Kinjo, M. Ichinohe, *Science* **2004**, *305*, 1755 – 1757.
[18] K. Abersfelder, A. J. P. White, H. S. Rzepa, D. Scheschkewitz, *Science* **2010**, *327*, 564 – 566.
[19] M. Weidenbruch, S. Willms, W. Saak, G. Henkel, *Angew. Chem. Int. Ed. Engl.* **1997**, *36*, 2503 – 2504; *Angew. Chem.* **1997**, *109*, 2612 – 2613.
[20] S. Inoue, J. D. Epping, E. Irran, M. Driess, *J. Am. Chem. Soc.* **2011**, *133*, 8514 – 8517.
[21] Y. Xiong, S. Yao, M. Driess, *Angew. Chem. Int. Ed.* **2013**, *52*, 4302 – 4311; *Angew. Chem.* **2013**, *125*, 4398 – 4407.
[22] A. C. Filippou, B. Baars, O. Chernov, Y. N. Lebedev, G. Schnakenburg, *Angew. Chem. Int. Ed.* **2014**, *53*, 565 – 570; *Angew. Chem.* **2014**, *126*, 576 – 581.
[23] R. Kobayashi, S. Ishida, T. Iwamoto, *Angew. Chem. Int. Ed.* **2019**, *58*, 9425 – 9428; *Angew. Chem.* **2019**, *131*, 9525 – 9528.
[24] S. Yao, Y. Xiong, M. Brym, M. Driess, *J. Am. Chem. Soc.* **2007**, *129*, 7268 – 7269.
[25] J. D. Epping, S. Yao, M. Karni, Y. Apeloig, M. Driess, *J. Am. Chem. Soc.* **2010**, *132*, 5443 – 5455.
[26] Y. Xiong, S. Yao, M. Driess, *Angew. Chem. Int. Ed.* **2010**, *49*, 6642 – 6645; *Angew. Chem.* **2010**, *122*, 6792 – 6795.
[27] Y. Xiong, S. Yao, R. Müller, M. Kaupp, M. Driess, *J. Am. Chem. Soc.* **2010**, *132*, 6912 – 6913.
[28] S. Yao, M. Brym, C. van Wüllen, M. Driess, *Angew. Chem. Int. Ed.* **2007**, *46*, 4159 – 4162; *Angew. Chem.* **2007**, *119*, 4237 – 4240.
[29] C. B. Yildiz, K. I. Leszczyńska, S. González-Gallardo, M. Zimmer, A. Azizoglu, T. Biskup, C. W. M. Kay, V. Huch, H. S. Rzepa, D. Scheschkewitz, *Angew. Chem. Int. Ed.* **2020**, *59*, 15087 – 15092; *Angew. Chem.* **2020**, *132*, 15199 – 15204.
[30] F. Weinhold, R. West, *Organometallics* **2011**, *30*, 5815 – 5824.
[31] F. Weinhold, R. West, *J. Am. Chem. Soc.* **2013**, *135*, 5762 – 5767.
[32] J. S. Ritch, T. Chivers, *Angew. Chem. Int. Ed.* **2007**, *46*, 4610 – 4613; *Angew. Chem.* **2007**, *119*, 4694 – 4697.
[33] I. T. Moraru, P. M. Petrar, G. Nemeş, *J. Phys. Chem. A* **2017**, *121*, 2515 – 2522.
[34] R. J. Gillespie, E. A. Robinson, *Chem. Soc. Rev.* **2005**, *34*, 396.
[35] T. S. Cameron, A. Decken, I. Krossing, J. Passmore, J. M. Rautiainen, X. Wang, X. Zeng, *Inorg. Chem.* **2013**, *52*, 3113 – 3126.
[36] J. Passmore, J. M. Rautiainen, *Eur. J. Inorg. Chem.* **2012**, 6002 – 6010.
[37] M. Fugel, M. F. Hesse, R. Pal, J. Beckmann, D. Jayatilaka, M. J. Turner, A. Karton, P. Bultinck, G. S. Chandler, S. Grabowsky, *Chem. Eur. J.* **2018**, *24*, 15275 – 15286.
[38] M. R. Churchill, C. H. Lake, S.-H. L. Chao, O. T. Beachley, *J. Chem. Soc. Chem. Commun.* **1993**, 1577 – 1578.
[39] C. Eaborn, P. B. Hitchcock, K. Izod, J. D. Smith, *Angew. Chem. Int. Ed. Engl.* **1996**, *34*, 2679 – 2680.
[40] A. Decken, J. Passmore, X. Wang, *Angew. Chem. Int. Ed.* **2006**, *45*, 2773 – 2777; *Angew. Chem.* **2006**, *118*, 2839 – 2843.

[41] A. Decken, F. A. LeBlanc, J. Passmore, X. Wang, *Eur. J. Inorg. Chem.* **2006**, 4033 – 4036.
[42] R. D. Ernst, A. Glöckner, A. M. Arif, *Z. Kristallogr. New Cryst. Struct.* **2007**, *222*, 333 – 334.
[43] I. Sänger, M. Gärtner, M. Bolte, M. Wagner, H.-W. Lerner, *Z. Anorg. Allg. Chem.* **2018**, *644*, 925 – 929.
[44] F. Dankert, C. von Hänisch, *Inorg. Chem.* **2019**, *58*, 3518 – 3526.
[45] F. Dankert, F. Weigend, C. von Hänisch, *Inorg. Chem.* **2019**, *58*, 15417 – 15422.
[46] F. Dankert, L. Erlemeier, C. Ritter, C. von Hänisch, *Inorg. Chem. Front.* **2020**, *7*, 2138 – 2153.
[47] F. Dankert, J. Heine, J. Rienmüller, C. von Hänisch, *CrystEngComm* **2018**, *20*, 5370 – 5376.
[48] J. Pahl, H. Elsen, A. Friedrich, S. Harder, *Chem. Commun.* **2018**, *54*, 7846 – 7849.
[49] M. Ouchi, Y. Inoue, T. Kanzaki, T. Hakushi, *Bull. Chem. Soc. Jpn.* **1984**, *57*, 887 – 888.
[50] Y. Inoue, M. Ouchi, T. Hakushi, *Bull. Chem. Soc. Jpn.* **1985**, *58*, 525 – 530.
[51] K. Reuter, M. R. Buchner, G. Thiele, C. von Hänisch, *Inorg. Chem.* **2016**, *55*, 4441 – 4447.
[52] K. Reuter, G. Thiele, T. Hafner, F. Uhlig, C. von Hänisch, *Chem. Commun.* **2016**, *52*, 13265 – 13268.
[53] K. Reuter, F. Dankert, C. Donsbach, C. von Hänisch, *Inorganics* **2017**, *5*, 11.
[54] F. Dankert, K. Reuter, C. Donsbach, C. von Hänisch, *Dalton Trans.* **2017**, *46*, 8727 – 8735.
[55] F. Dankert, C. Donsbach, C.-N. Mais, K. Reuter, C. von Hänisch, *Inorg. Chem.* **2018**, *57*, 351 – 359.
[56] F. Dankert, K. Reuter, C. Donsbach, C. von Hänisch, *Inorganics* **2018**, *6*, 15.
[57] M. R. Buchner, M. Müller, F. Dankert, K. Reuter, C. von Hänisch, *Dalton Trans.* **2018**, *47*, 16393 – 16397.
[58] F. Dankert, C. Donsbach, J. Rienmüller, R. M. Richter, C. von Hänisch, *Chem. Eur. J.* **2019**, *25*, 15934 – 15943.
[59] J. Chojnowski, J. Kurjata, *Macromolecules* **1994**, *27*, 2302 – 2309.
[60] L.-C. Pop, M. Saito, *Coord. Chem. Rev.* **2016**, *314*, 64 – 70.
[61] I. Haiduc, *Organometallics* **2004**, *23*, 3 – 8.
[62] M. Cypryk, J. Kurjata, J. Chojnowski, *J. Organomet. Chem.* **2003**, *686*, 373 – 378.
[63] M. Cypryk, *Macromol. Theory Simul.* **2001**, *10*, 158 – 164.
[64] G. W. Buchanan, M. F. Rastegar, G. P. A. Yap, *J. Mol. Struct.* **2002**, *605*, 1 – 8.
[65] R. D. Shannon, *Acta Crystallogr. Sect. A* **1976**, *32*, 751 – 767.
[66] J. C. Chambron, M. Meyer, *Chem. Soc. Rev.* **2009**, *38*, 1663 – 1673.
[67] I. Krossing, A. Reisinger, *Eur. J. Inorg. Chem.* **2005**, 1979 – 1989.
[68] D. Stasko, S. P. Hoffmann, K. C. Kim, N. L. P. Fackler, A. S. Larsen, T. Drovetskaya, F. S. Tham, C. A. Reed, C. E. F. Rickard, P. D. W. Boyd, E. S. Stoyanov, *J. Am. Chem. Soc.* **2002**, *124*, 13869 – 13876.
[69] P. Jutzi, C. Müller, A. Stammler, H. G. Stammler, *Organometallics* **2000**, *19*, 1442 – 1444.
[70] M. Morisue, T. Kusukawa, S. Watase, *Eur. J. Inorg. Chem.* **2020**, 1885 – 1893.
[71] R. F. Weitkamp, B. Neumann, H. Stammler, B. Hoge, *Angew. Chem. Int. Ed.* **2020**, *59*, 5494 – 5499; *Angew. Chem.* **2020**, *132*, 5536 – 5541.
[72] M. Ichinohe, N. Takahashi, A. Sekiguchi, *Chem. Lett.* **1999**, *28*, 553 – 554.
[73] A. Schäfer, M. Reißmann, A. Schäfer, M. Schmidtmann, T. Müller, *Chem. Eur. J.* **2014**, *20*, 9381 – 9386.
[74] Z. M. Tun, M. J. Panzner, V. Scionti, D. Medvetz, C. Wesdemiotis, W. J. Youngs, C. Tessier, *J. Am. Chem. Soc.* **2010**, *132*, 17059 – 17061.
[75] X. Xie, C. Auel, W. Henze, R. M. Gschwind, *J. Am. Chem. Soc.* **2003**, *125*, 1595 – 1601.
[76] R. Neufeld, M. John, D. Stalke, *Angew. Chem. Int. Ed.* **2015**, *54*, 6994 – 6998; *Angew. Chem.* **2015**, *127*, 7100 – 7104.
[77] J. E. Tanner, *Chem. Phys.* **1970**, *52*, 2523 – 2526.
[78] C. S. Johnson, *Prog. Nucl. Magn. Reson. Spectrosc.* **1999**, *34*, 203 – 256.
[79] D. Ben-Amotz, K. G. Willis, *J. Phys. Chem.* **1993**, *97*, 7736 – 7742.
[80] F. Dankert, H. L. Deubner, M. Müller, M. R. Buchner, F. Kraus, C. von Hänisch, *Z. Anorg. Allg. Chem.* **2020**, *646*, 1501 – 1507.
[81] TURBOMOLE V7.5 2020, a development of University of Karlsruhe and Forschungszentrum Karlsruhe GmbH, 1989 – 2007, TURBOMOLE GmbH, since 2007; available from http://www.turbomole.com.
[82] J. Perdew, K. Burke, M. Ernzerhof, *Phys. Rev. Lett.* **1996**, *77*, 3865 – 3868.
[83] F. Weigend, R. Ahlrichs, *Phys. Chem. Chem. Phys.* **2005**, *7*, 3297 – 3305.
[84] A. Klamt, G. Schüürmann, *J. Chem. Soc. Perkin Trans. 2* **1993**, 799 – 805.
[85] P. Plessow, *J. Chem. Theory Comput.* **2013**, *9*, 1305 – 1310.
[86] Deposition Numbers 2035390 (**I**), 2035394 (**II**·0.5 DCM), 2035392 (**1**), 2035388 (**2**), 2035391 (**4**·2 DCM), 2035387 (**4a**), 2035396 (**5**), 2035389 (**6**) 2035393 (**S1**), and 2035395 (**S2**) contain the supplementary crystallographic data for this paper. These data are provided free of charge by the joint Cambridge Crystallographic Data Centre and Fachinformationszentrum Karlsruhe Access Structures service www.ccdc.cam.ac.uk/structures.

Manuscript received: November 18, 2020
Revised manuscript received: February 1, 2021
Accepted manuscript online: February 16, 2021
Version of record online: March 23, 2021

